Acta Chimica Slovaca, Vol.1, No. 1, 2008, 72 – 84

Quantum-chemical study of N,N´-diphenyl-p-phenylenediamine (DPPD) dehydrogenation

Anton Gatial*, Júlia Polovková[a] , Martin Breza

Institute of Physical Chemistry and Chemical Physics, Slovak University of Technology, SK-81237 Bratislava, Slovakia
[a]Institute of Measurement Science, Slovak Academy of Sciences, SK-84104 Bratislava, Slovakia

[*]anton.gatial@stuba.sk

In the memory of Professor Vojtech Kellö (1919–2007)

Abstract

Using B3LYP/6-31G* treatment, the optimal geometries and IR spectra of N,N´-diphenyl-p-phenylenediamine antioxidant (DPPD) and of N,N´-diphenyl-p-quinonediimine (DQDI) as its double dehydrogenated oxidation product have been obtained. The complete conformation analysis predicts the existence of four stable conformers of each of the systems under study. Experimental IR spectra of DPPD sample heated on air at 140 ºC confirmed the DQDI formation even at increased temperatures.

Keywords: Antioxidants; N,N´-substituted *p*-phenylenediamines; dehydrogenated structures; IR spectra; DFT geometry optimization.

Introduction

Aromatic secondary amines, particularly N,N´-substituted *p*-phenylenediamines (PPD), represent the most important group of antioxidants used in rubber industry (Cataldo 2001, 2002). Antioxidants reduce the concentration of radicals that determines the rate of the oxidation reaction. It is supposed that benzoquinonediimines are reaction products of PPD degradation. EPR spectroscopy confirmed the formation of aminyl radicals and especially the nitroxide radicals originating from the -NH- bridge oxidation by $ROO^{\bullet}$ radicals (Landolt-Börnstein 1980a, 1980b, Male 1988, Petr 1988, Omelka 2001, Burian 2003).

On the other hand, non-isothermal DSC studies of the antioxidant effectiveness of a series of N-alkyl-N´-aryl-*p*-phenylenediamines in polyisoprene rubber (Cibulková 2005a,

2005b) indicate the existence of the ketimine structures instead of the classical benzoquinonediimine-type ones. This conclusion has been confirmed by our IR spectra measurements of N-phenyl-N´-isopropyl-p-phenylenediamine (IPPD) (Polovková 2006) and N-phenyl-N´-(1´-methylbenzyl)-p-phenylenediamine (SPPD) (Gatial 2007) supported by DFT calculations (Polovková 2006, Gatial 2007, Breza 2006). According to our results, IR spectra of the samples heated on air at 140 ºC correspond to the double dehydrogenated structures with the Phenyl-N=C ketimine double bond and not to their N,N´-dehydrogenated quinonediimine-type counterparts. In this sense the FTIR spectral studies of thermal aging of polyisoprene rubber with different concentrations of the N-phenyl-N´-1,3-dimethyl-butyl-p-phenylenediamine (6PPD) antioxidant in hot air at 140 ^{o}C (Li 2003) demand new interpretation as well (a broad band observed at 1670 cm^{-1} cannot be ascribed to the C=N stretching of a quinonediimine-type structure).

The physico-chemical properties of N,N´-diphenyl-p-phenylenediamine (DPPD) have been object of many studies (Shacklette 1988, Choi 1999, Zheng 1994, Quillard 2001, 2003, Boyer 1998, 2000a, Nishiumi 2003, de Santana 2006, Boozer 1955, Howard 1973). According to EPR measurements in solution at room temperature, it reacts with peroxy radicals to give N,N´-diphenyl-p-quinonediimine (DQDI). No degradation studies of DPPD antioxidant at high temperature are known in the literature. To complete the above mentioned studies of PPD antioxidants degradation at high temperatures, an analogous study of DPPD is to be performed because the double dehydrogenated degradation product of this compound cannot correspond to a ketimine structure. Analogously to room temperature oxidation in solution, the formation of DQDI only may be supposed as well. As the IR spectra of DQDI are well known (see above), it is not necessary to isolate the degradation product. The aim of our study is to identify the structure of the DPPD double dehydrogenation products at high temperatures – whether the observed IR spectra really correspond to DQDI or not. We want neither to isolate the degradation product nor to determine the degradation degree – there are other analytic methods which are more suitable for this purpose (such as chromatography). The geometry of all DPPD and DQDI conformers will be optimized and the measured vibration spectra of the degraded sample will be interpreted using quantum chemistry treatment. In this study the side benzene rings are denoted as Ph1 and Ph3, respectively, and the central 1,4-disubstituted ring as Ph2.

Experimental

IR measurements

A powder sample of N,N´-diphenyl-p-phenylenediamine has been purchased by Merck-Schuchardt and used as received. Transmission mid-infrared spectra (4000-400 cm^{-1}) at room temperature were collected by Nicolet model NEXUS 470 FTIR spectrometer using standard KBr technique. The sample (ca 2 g) was placed on a glass dish and heated in an oven at 140 °C on air until the evident formation of dark colored oxidation products occurred (approx. 2 days). FTIR spectra of such treated sample were taken for various thermal degradation times.

Quantum-chemical calculations

Standard B3LYP/6-31G* geometry optimizations of four possible conformations of N,N´-diphenyl-p-phenylenediamine (DPPD, models A1, B1, C1 and D1, see Figs. 1 - 4 and Table 1) and of its doubly dehydrogenated DQDI products at both N sites in singlet (spin multiplicity $M_S = 1$, models A2, B2, C2 and D2, see Table 1) and triplet spin ground states ($M_S = 3$, models A3, B3, C3 and D3, see Table 1) have been performed using Gaussian03 program package (Frisch 2003). In the next step, the vibrational frequencies of the above mentioned molecules have been computed and compared with the experimental ones. Calculated DFT vibrational frequencies have been scaled by the factor of 0.9614 (Scott 1996). A potential energy distribution (PED) analysis has been performed as well.

Results and Discussion

Whereas in the first DPPD dehydrogenation step only simple radicals ($M_S = 2$) may be formed, the products of its second dehydrogenation step may have either no ($M_S = 1$) or two (a biradical, $M_S = 3$) unpaired electrons. In the conformers notation (Table 1), the first symbol (syn- or anti-) denotes mutual orientations of N-C bonds connecting the side rings and the second one denotes mutual orientation of the side rings planes (syn- for parallel and gauche-

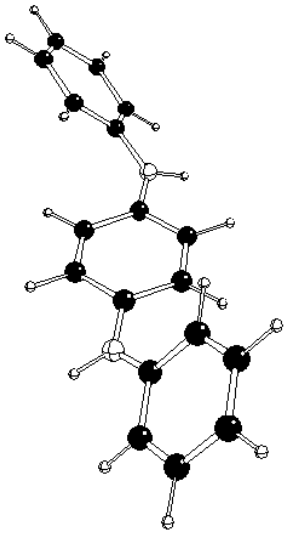

Fig. 1. Optimal geometry of anti, gauche-conformation of DPPD (model A1).

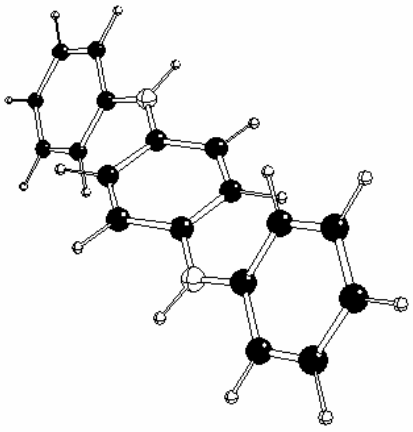

Fig. 2. Optimal geometry of anti, syn-conformation of DPPD (model B1).

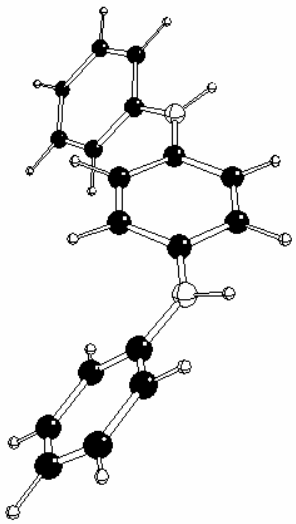

Fig. 3. Optimal geometry of syn, syn-conformation of DPPD (model C1).

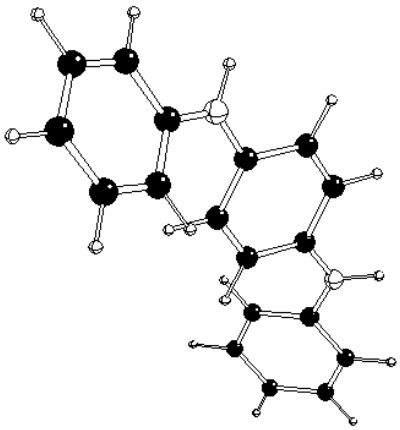

Fig. 4. Optimal geometry of syn, gauche-conformation of DPPD (model D1).

Table 1. Notation of DPPD and DQDI model systems

Model	System	Conformation[a)]	Symmetry	Spin multiplicity M_S
A1	DPPD	anti, gauche-	C_2	1
A2	DQDI			1
A3	DQDI			3
B1	DPPD	anti, syn-	C_i	1
B2	DQDI			1
B3	DQDI			3
C1	DPPD	syn, syn-	C_s	1
C2	DQDI			1
C3	DQDI			3
D1	DPPD	syn, gauche-	C_2	1
D2	DQDI			1
D3	DQDI			3

[a)] the first symbol denotes mutual orientations of N-C bonds and the second one denotes the mutual orientation of the side rings planes

Table 2. Energy parameters of DPPD and DQDI model systems

Model	M_S	E_{tot} / (hartree)	E_{tot} + ZPE / (hartree)	$\Delta(E_{tot} + ZPE)$[a)] / (kJ/mol)
DPPD systems				
A1	1	-805.05333	-804.75767	0.0
B1	1	-805.05316	-804.75759	0.2
C1	1	-805.05311	-804.75748	0.5
D1	1	-805.05319	-804.75753	0.4
DQDI systems				
A2	1	-803.81073	-803.53879	0.0
A3	3	-803.77676	-803.50736	82.5
B2	1	-803.81065	-803.53871	0.2
B3	3	-803.77684	-803.50742	82.4
C2	1	-803.81076	-803.53873	0.2
C3	3	-803.77656	-803.50718	83.0
D2	1	-803.81012	-803.53812	1.8
D3	3	-803.77681	-803.50747	82.2

[a)] related to A1 (DPPD systems) or A2 (DQDI systems) model system

for declined side rings planes). It must be mentioned that whereas Choi et al. (Choi 1999) have found only two stable DQDI conformers at B3LYP/6-31G* level of theory, we have found four stable DPPD and DQDI conformers of different energies that are not symmetry related (see Figs. 1-4 and Tables 1 and 2).

The total energy data without (E_{tot}) as well as with zero-point energy corrections (E_{tot} + ZPE) for our model systems are summarized in Table 2. Among the DPPD and DQDI model systems in the singlet spin state, the anti, gauche-conformers are the most stable structures (A1 and A2 model systems, respectively) and syn, gauche-conformations (D1 and D2 model systems, respectively) exhibit the least stability whereas the DQDI biradicals (M_S = 3) exhibit the reverse trend. Nevertheless, the singlet-triplet separation is over 80 kJ/mol in all cases and it indicates only vanishing concentrations of biradicals in equilibrium even at higher temperatures.

The energy differences between individual DPPD conformers are very small and it implies their simultaneous existence in real systems. Nevertheless, their IR spectra are so similar that we can restrict to the most stable A1 conformer in their discussion. The same holds for DQDI systems in singlet spin state. The existence of various DPPD and DQDI conformers in real systems has been confirmed by X-ray structure data (Quillard 2001, Potevyeva 1976, Boyer 2000b, Baughman 1988).

Survey IR spectra of unheated DPPD in KBr pellet together with IR spectra of its oxidized state after 5 days thermal treatment in the hot air at 140 ºC are shown in Fig. 5 and Table 3. The IR spectrum of unheated DPPD has the features which are more typical for crystalline state and its IR spectrum is available elsewhere (Cochet 2000, Boyer 1998, Quillard 1992, 1994). On the other side the spectra after hot air acting are more alike to the amorphous state with broad bands. This reflects the fact that DPPD is molten at 140 ºC. During hot air acting on DPPD many split bands became broader and combined into one band with changed intensity. In general, both spectra (before and after thermal treatment) are similar and only few bands in IR spectra almost disappeared or decreased their intensity (for instance the bands around 3388, 1533, 1522, 1333, 1311, 1224, 1177 and 875 cm^{-1}) and some new bands arose which can be assigned to the oxidized products (see for example bands at 1264 cm^{-1} and 1108 cm^{-1} which are marked by asterisks in Fig. 6). In the similar studies of 6PPD (Li 2003), IPPD (Polovková 2006), and SPPD (Gatial 2007), in the region of the double bonds stretching vibration the most dramatic changes were observed and a new very strong band around 1660 cm^{-1} appeared. Such changes in the IR spectra of DPPD are not visible and the mentioned band was not observed (Fig. 7).

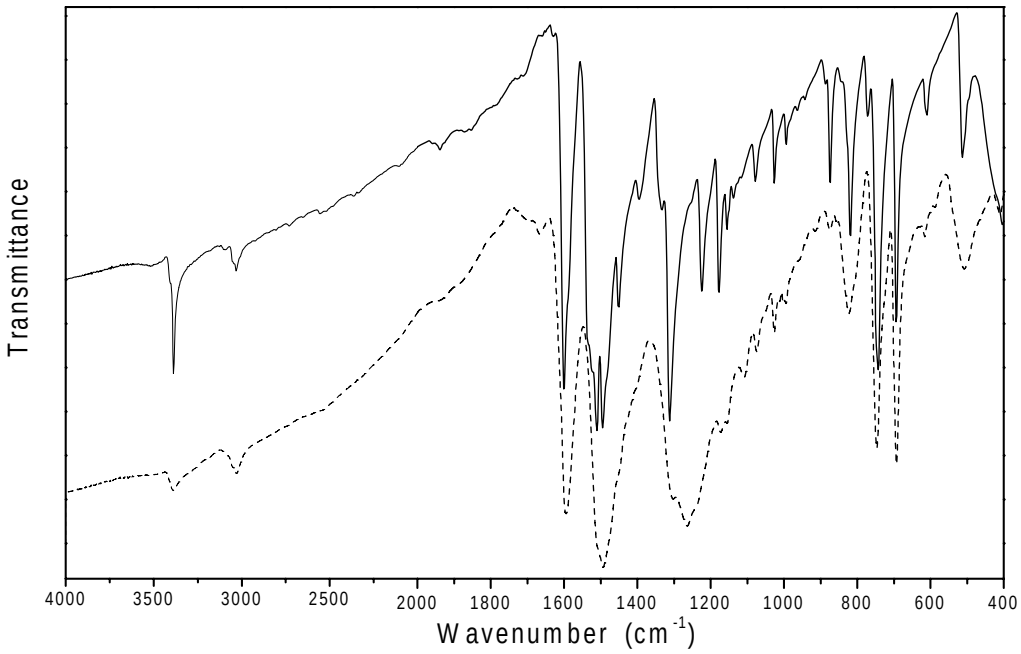

Fig. 5. IR spectra of DPPD in KBr pellet before (full line) and after heating at 140 °C on air for 5 days (dotted line).

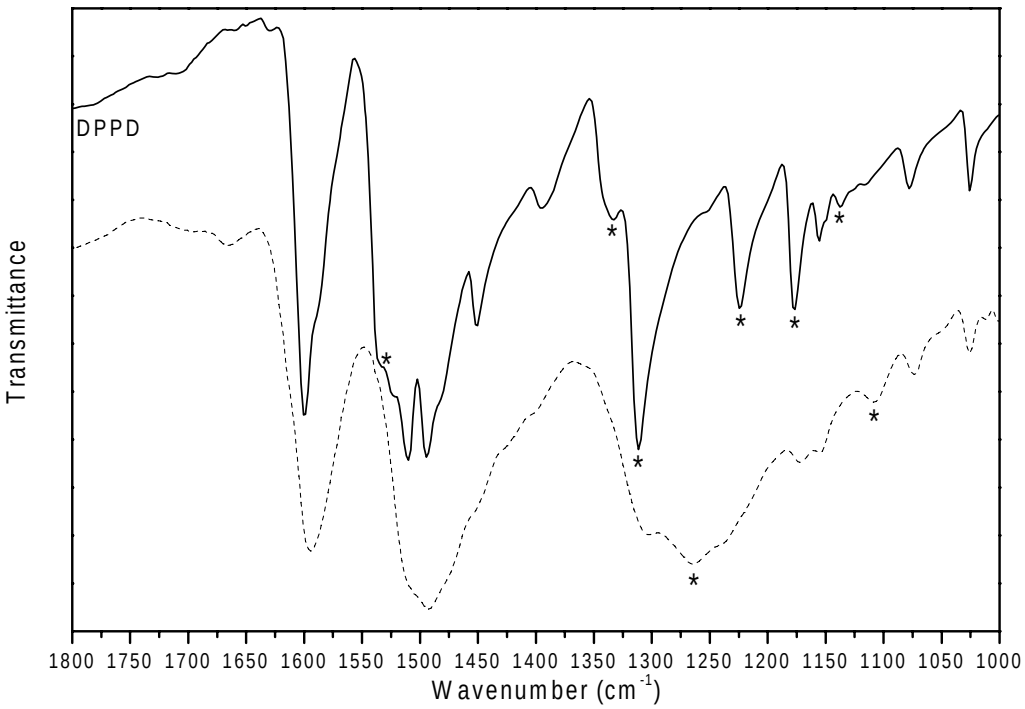

Fig. 6. Detail of Fig. 5.

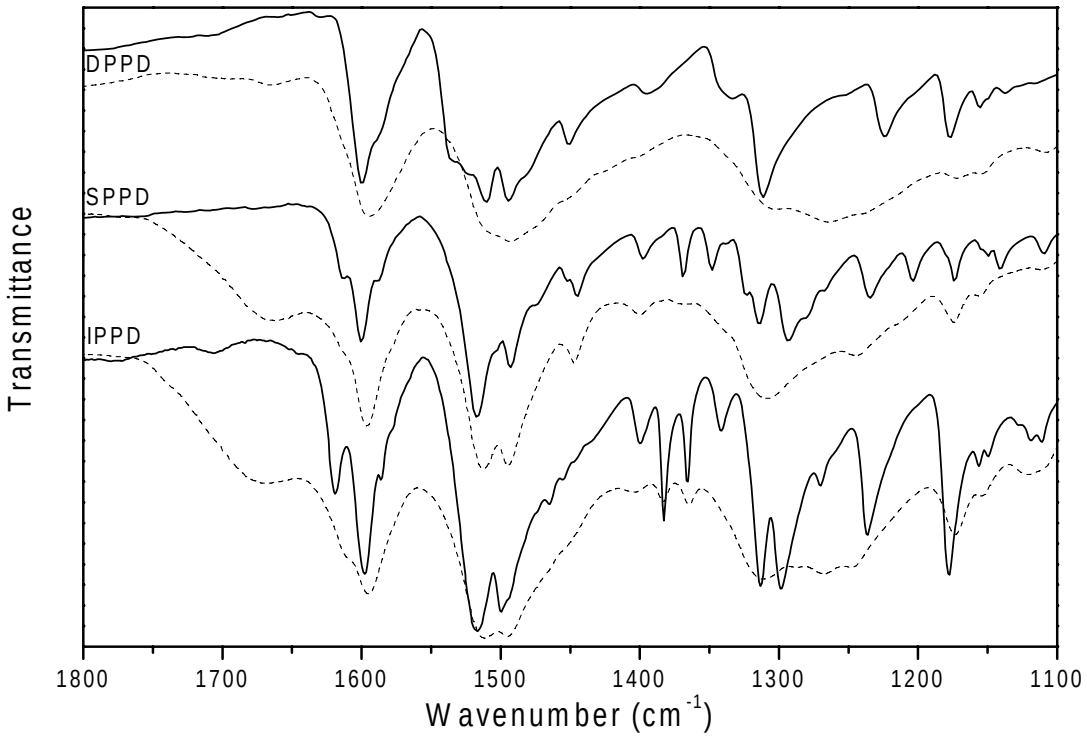

Fig. 7. Comparison of DPPD, SPPD and IPPD IR spectra in KBr pellet before (full lines) and after heating (dotted lines).

The appearing of the new band at 1660 cm^{-1} in the IR spectrum of SPPD and IPPD was explained by the formation of the Phenyl-N_B=C- ketimine structure in singlet spin state during their oxidation and not of its N,N´-dehydrogenated quinonediimine-type structure as supposed in the literature (Li 2003) for 6PPD. In 6PPD, SPPD and IPPD the formation of the ketimine structure is possible because amino-nitrogen is bonded with the secondary carbon. On the other side, the formation of the ketimine structure is not possible in DPPD and therefore the appearing of the new band at 1660 cm^{-1} in its IR spectrum is impossible in agreement with the experimental results.

During the thermal dehydrogenation of DPPD the splitting-off the hydrogen from the both amino-nitrogen atoms and creation of the DQDI is supposed. This can be supported by the strong decrease of the intensity of the N-H stretching vibration band at 3388 cm^{-1} in comparison with the C-H stretching bands and by the disappearing of the bands at 1533 and 1522 cm^{-1} which are assigned to NH deformation modes according to the PED calculations.

Table 3. DFT calculated vibrational frequencies, IR intensities and bands assignment for DPPD and DQDI

DPPD				DQDI		
ν_{scaled} [a]	Intensity [b]	Assignment [c]	ν_{exp} [d]	ν_{scaled} [a]	Intensity [b]	Assignment [c]
				1632	0.0	C=C *s*s (Ph2)
1615	0.07	CC s (8a, Ph2)				
1601	23.6	CC s (8a, Ph1, Ph3 s)	1600 vs	1598	17.9	CC s (8a, Ph1, Ph3 a)
1600	329.7	CC s (8a, Ph1, Ph3 a)	1590 s,sh	1587	0.1	CC s (8a, Ph1, Ph3 s)
1584	1.7	CC s (8b, Ph1, Ph3 s)				
1582	44.6	CC s (8b, Ph1, Ph3 a)	1575 w,sh			
1571	3.6	CC s (8b, Ph2)		1576	99.0	C=N *a*s
				1567	18.4	C=C *a*s (Ph2)
				1562	2.9	CC s (8b, Ph1, Ph3 a)
				1562	4.0	CC s (8b, Ph1, Ph3 s)
				1528	0.1	C=N *s*s
1516	848.5	NH *a*δ	1533 m			
			1522 m			
1501	78.7	CC s (19a, Ph2)	1510 vs			
1498	32.4	NH *s*δ	1494 s			
1485	393.1	CC s (19a, Ph1, Ph3 a)	1484 s,sh	1472	50.0	CC s (19a, Ph1, Ph3 a)
1483	0.03	CC s (19a, Ph1, Ph3 s)		1470	1.0	CC s (19a, Ph1, Ph3 s)
1446	6.3	CC s (19b, Ph1, Ph3 a)	1451 m	1437	2.0	CC s (19b, Ph1, Ph3 a)
1421	2.5	CC s (19b, Ph1, Ph3 s)		1436	2.2	CC s (19b, Ph1, Ph3 s)
1390	33.7	CC s (19b, Ph2)	1395 w	1393	0.0	C-C s (Ph2)
				1374	1.2	CCH δ (Ph2)
1327	0.7	CC s (14, Ph1, Ph3, s)				
1321	100.5	CC s (14, Ph1, Ph3, a)	1333 m	1310	0.8	CC s (14, Ph1, Ph3 a)
1317	2.0	CCH δ (3, Ph1, Ph3)		1310	0.0	CC s (14, Ph1, Ph3 s)
				1296	15.8	C-C s (Ph2)
1304	122.9	CCH δ (3, Ph1, Ph3)	1311 s			
1302	4.5	CCH δ (3, Ph2)				
1300	519.3	C-N_A-C *a*s, CC s (14, Ph2)	1293 m,sh			
				1281	0.0	CCH δ (3, Ph1, Ph3)
				1273	2.6	CCH δ (3, Ph1, Ph3)
1245	1.2	CC s (14, Ph2), C-N_A-C *a*s	1252 vw	1242	0.1	CCH δ (Ph2)
1224	79.1	C-N_A-C *a*s	1224 m			
1213	19.8	C-N_A-C *s*s	1202 w,sh	1208	0.04	N_A-C *s*s
1210	3.1	C-N_A-C *s*s		1204	35.4	N_A-C *a*s
1171	2.4	CCH δ (9a Ph2)		1157	1.3	CCH δ (9a, Ph1, Ph3)
1168	22.8	CCH δ (9a Ph1, Ph3)	1177 m	1156	0.1	CCH δ (9a, Ph1, Ph3)
1166	0.1	CCH δ (9a Ph1, Ph3)	1156 w	1151	0.4	CCH δ (Ph2)
1145	1.2	CCH δ (9b Ph1, Ph3)	1150 w,sh	1145	0.5	CCH δ (9b, Ph1, Ph3)
1145	1.7	CCH δ (9b Ph1, Ph3)	1137 vw	1145	0.2	CCH δ (9b, Ph1, Ph3)
1111	11.33	CCH δ (15 Ph2)	1116 vw			
				1089	24.5	CCH δ (Ph2)
1075	5.0	CCH δ (15 Ph1, Ph3)	1078 w	1067	6.2	CCH δ (15, Ph1, Ph3)
1074	1.8	CCH δ (15 Ph1, Ph3)		1066	2.8	CCH δ (15, Ph1, Ph3)

Table 3. (cont.)

DPPD				DQDI		
ν_{scaled} [a]	Intensity [b]	Assignment [c]	ν_{exp} [d]	ν_{scaled} [a]	Intensity [b]	Assignment [c]
				1632	0.0	C=C *ss* (Ph2)
1018	0.6	CCH δ (18a Ph1, Ph3)	1026 m	1013	6.3	CCH δ (18a, Ph1, Ph3)
1018	7.0	CCH δ (18a Ph1, Ph3)	1011 vw,sh	1013	0.1	CCH δ (18a, Ph1, Ph3)
990	0.1	CCH δ (18a Ph2)	993 m			
				983	0.2	CCH wa (Ph2)
972	0.4	CC s (1, Ph1, Ph3)	985 w,sh	974	0.1	CC s (1, Ph1, Ph3)
972	8.6	CC s (1, Ph1, Ph3)		974	3.5	CC s (1, Ph1, Ph3)
				972	0.1	CCH wa (Ph2)
944	1.3	CCH wa (5, Ph1, Ph3)	963 vw	952	0.7	CCH wa (5, Ph1, Ph3)
944	0.1	CCH wa (5, Ph1, Ph3)		952	0.1	CCH wa (5, Ph1, Ph3)
922	0.1	CCH wa (17a, Ph1, Ph3)	942 vw			
922	0.1	CCH wa (17a, Ph1, Ph3)		935	3.0	CCC δ (Ph2)
911	1.4	CCH wa (5, Ph2)		928	0.02	CCH wa (17a, Ph1, Ph3)
909	0.2	CCH wa (17a, Ph2)	886 vw	928	4.1	CCH wa (17a, Ph1, Ph3)
				887	0.8	CCH wa (17b, Ph1, Ph3)
				886	13.3	CCH wa (17b, Ph1, Ph3)
869	0.1	CC ss (1, Ph2)				
858	16.6	CCC δ (12, Ph1, Ph3)	874 s	851	43.0	CCH wa (Ph2)
858	1.2	CCH wa (17b, Ph1, Ph3)		848	7.0	C-C s (Ph2)
857	4.1	CCH wa (17b, Ph1, Ph3)	842 vw			
823	20.5	CCC δ (12, Ph1, Ph3)	828 w,sh	833	2.5	CC *ss* (1, Ph2)
810	0.8	CCH wa (10a, Ph1, Ph3)		819	15.1	CCH wa (10a, Ph1, Ph3)
807	10.7	CCH wa (10a, Ph1, Ph3)	819 vs	817	0.7	CCH wa (10a, Ph1, Ph3)
793	14.1	CCH wa (11, Ph2)		776	3.2	CCH wa (Ph2)
791	5.0	CCH wa (10a, Ph2)		775	11.4	CCC δ (Ph1, Ph3)
768	2.8	CCC δ (12, Ph2)	771 w	765	46.1	CCC δ (Ph1, Ph3)
733	59.4	CCH wa (11, Ph1, Ph3)	742 vs	738	16.8	CCH wa (11, Ph1, Ph3)
728	40.0	CCH wa (11, Ph1, Ph3)		737	14.0	CCH wa (11, Ph1, Ph3)

[a] Frequency in cm^{-1} and scaled by the scale factor 0.9614.
[b] In unit km/mol.
[c] s stretch; δ deformation; wa wagging; *s* symmetric; *a* asymmetric;
[d] s strong; m medium; w weak; v very; sh shoulder;

The most significant changes between both spectra are in the 1350-1200 cm^{-1} region. In the 1350-1250 cm^{-1} region the bands of CC ring stretch mode (denoted as mode 14 according to the Wilson's notation) and CCH ring deformation mode (mode 3) can be expected and in the 1200-1300 cm^{-1} region the C-N-C asymmetric and symmetric stretch vibrations. For 1,4-disubstituted benzene ring these modes are at about 10-15 cm^{-1} lower frequencies than for the monosubstituted ones (Roeges 1994). In ref. (Boyer 1998), the one of the most strongest bands in IR spectra of DPPD around 1300 cm^{-1} was not assigned to some vibrational mode because no intense band was predicted by the calculation in this area and it was interpreted as a coupling between mode 14 and C-N-C asymmetric stretching vibration. However, in our

calculations this band was evaluated as the second most intense band at 1300 cm^{-1} and according PED really corresponds to the mode 14 of the 1,4-disubstituted Ph2 benzene ring and C-N-C asymmetric stretching vibration. Also the DPPD band at 1224 cm^{-1}, which dramatically changes its intensity, is according to PED connected with the C-N-C asymmetric stretching vibration. During the transformation of DPPD to DQDI the Ph2 benzene ring is converted to a benzoquinone ring and two C=N double bonds are created. Therefore it is not surprising that after thermal treatment both mentioned bands decrease their intensity and the appearing new band at 1264 cm^{-1} can be ascribed to DQDI (Boyer 1998).

Also decreasing intensity of the DPPD band at 1177 cm^{-1} is in agreement with the calculated ca 15 cm^{-1} downshift of the CCH deformation modes (mode 9a) for all three benzene rings and the calculated decrease of its intensities.

Finally it may be concluded that our results confirmed the formation of quinonediimine type structures of DQDI (without any complicated products isolation) even during DPPD heating on air at 140 ºC unlike N-alkyl-N'-aryl-p-phenylenediamines (such as IPPD and SPPD) which are degraded to ketimine structures (Polovková 2006, Gatial 2007). Moreover, the complete quantum-chemical interpretation of IR spectra of DPPD and DQDI has been elaborated. Nevertheless, further experimental as well as theoretical studies are desirable to explain the complete mechanism of PPD antioxidants deterioration.

Acknowledgement

This work was supported by Science and Technology Assistance Agency under the contract No. APVV-20-0045-04. Slovak Grant Agency VEGA (contracts No. 1/3566/06 and 1/0535/08) is acknowledged for partial financial support. M.B. benefitted from the Centers of Excellence Programme of the Slovak Academy of Sciences in Bratislava, Slovakia (COMCHEM, contract no. II/1/2007). We thank NIC Juelich (Germany) for computing facilities.

References

Baughman RH, Wolf JF, Eckhardt H, Shacklette LW (1988) Synth. Met. 25: 121;

Boozer CE, Hammond GS, Sen JN (1955) J. Am. Chem. Soc. 77: 3233;

Boyer MI, Quillard S, Rebourt E, Louarn G, Buisson JP, Monkman A, Lefrant S (1998) J. Phys. Chem. B 102: 7382;

Boyer MI, Quillard S, Louarn G, Froyer G, Lefrant S (2000a) J. Phys. Chem. B 104: 8952.

Boyer MI, Quillard S, Corraze B, Deniard P, Evain M (2000b) Acta Crystallogr. C 56: e159;

Breza M, Kortišová I, Cibulková Z (2006) Polym. Degrad. Stab. 91: 2848;

Burian M, Omelka L, Ondrášová S, Brezová V (2003) Monatsh. Chem. 134: 501;

Cataldo F (2001) Polym. Degrad. Stab. 72: 787;

Cataldo F (2002) Eur. Polym. J. 38: 885;

Choi ChH, Kertesz M, Boyer MI, Cochet M, Quillard S, Louarn G, Lefrant S (1999) Chem. Mater. 11: 855;

Cibulková Z, Šimon P, Lehocký P, Balko J (2005a) J. Polym. Degrad. Stab. 87: 479;

Cibulková Z, Šimon P, Lehocký P, Balko J (2005b) J. Therm. Anal. Cal. 80: 357;

Cochet M, Louarn G, Quillard S, Boyer MI, Buisson JP, Lefrant S (2000) J. Raman Spectrosc. 31: 1029;

de Santana H, Quillard S, Fayad E, Louarn G (2006) Synth. Met. 156: 81;

Frisch MJ, Trucks GW, Schlegel HB, Scuseria GE, Robb MA, Cheeseman JR, Montgomery JA, Jr., Vreven T, Kudin KN, Burant JC, Millam JM, Iyengar SS, Tomasi J, Barone V, Mennucci B, Cossi M, Scalmani G, Rega N, Petersson GA, Nakatsuji H, Hada M, Ehara M, Toyota K, Fukuda R, Hasegawa J, Ishida M, Nakajima T, Honda Y, Kitao O, Nakai H, Klene M, Li X, Knox JE, Hratchian HP, Cross JB, Adamo C, Jaramillo J, Gomperts R, Stratmann RE, Yazyev O, Austin AJ, Cammi R, Pomelli C, Ochterski JW, Ayala PY, Morokuma K, Voth GA, Salvador P, Dannenberg JJ, Zakrzewski VG, Dapprich S, Daniels AD, Strain MC, Farkas O, Malick DK, Rabuck AD, Raghavachari K, Foresman JB, Ortiz JV, Cui Q, Baboul AG, Clifford S, Cioslowski J, Stefanov BB, Liu G, Liashenko A, Piskorz P, Komaromi I, Martin RL, Fox DJ, Keith T, Al-Laham MA, Peng CY, Nanayakkara A, Challacombe M, Gill PMW, Johnson B, Chen W, Wong MW, Gonzalez C, Pople JA (2003) *Gaussian 03*, Revision C.1. Gaussian, Inc., Pittsburgh (PA);

Gatial A, Polovková J, Kortišová I, Breza M. (2007) Vibr. Spectrosc. 44: 1;

Howard JA (1973). In: Kochi JK (Ed) Free radicals Vol. II (p. 51). J. Wiley, New York;

Landolt-Börnstein (1980a) New Series Vol. 9 Magnetic Properties of Free Radicals, Part c1, p. 556. Springer-Verlag, Berlin-Heidelberg-New York 1980;

Landolt-Börnstein (1980b) New Series Vol. 9 Magnetic Properties of Free Radicals, Part d2, p. 52. Springer-Verlag Berlin-Heidelberg-New York 1980;

Li GY, Koenig JL (2003) Polym. Degrad. Stab. 81: 377;

Male R, Allendorfer D (1988) J. Phys. Chem. 92: 6237;

Nishiumi T, Nomura Y, Higuchi M, Yamamoto K (2003) Chem. Phys. Lett. 378: 18;

Omelka L, Ondrášová S, Dunsch L, Petr A, Staško A (2001) Monatsh. Chem. 132: 597;

Petr A, Dunsch L (1988) J. Phys. Chem. 100: 6237;

Polovková J, Kortišová I, Gatial A, Breza M (2006) Polym. Degrad. Stab. 91: 1775;

Potevyeva ZP, Chetkina LA, Kopilov VV (1976) Kristallografiya 21: 312;

Quillard S, Louarn G, Buisson JP, Lefrant S, Masters J, Macdiarmid AG (1992) Synth. Met. 49: 525;

Quillard S, Louarn G, Lefrant S, Macdiarmid AG (1994) Phys. Rev. B 50: 12496;

Quillard S, Corraze B, Boyer MI, Fayad E, Louarn G, Froyer G (2001) J. Mol. Struct. 596:33;

Quillard S, Corraze B, Poncet M, Mevellec JY, Buisson JP, Evain M, Wang W, MacDiarmid AG (2003) Synth. Met. 137: 921;

Roeges NPG (1994) Guide to the interpretation of infrared spectra of organic structures. John Wiley & Sons, Chichester;

Scott AP, Radom L (1996) J. Phys. Chem. 100: 16502;

Shacklette LW, Wolf JF, Gould S, Baughman RH (1988) J. Chem. Phys. 88: 3955;

Zheng WY, Levon K, Laakso J, Oesterholm JE (1994) Macromol. 27: 7754;